Calcitonin-typical suppression of osteoclastic activity by amphioxus calcitonin superfamily peptides and insights into the evolutionary conservation and diversity of their structures

doi: 10.1016/j.ygcen.2017.01.004

Calcitonin-typical suppression of osteoclastic activity by amphioxus calcitonin superfamily peptides and insights into the evolutionary conservation and diversity of their structures

Toshio Sekiguchi[1], Akira Shiraishi[2], Honoo Satake[2], Kenji Kuwasako[3], Hiroki Takahashi[4], Masayuki Sato[1], Makoto Urata[1,5], Shuichi Wada[6], Masato Endo[7], Takahiro Ikari[1], Atsuhiko Hattori[8], Ajai K. Srivastav[9] and Nobuo Suzuki[1*]

[1]Noto Marine Laboratory, Institute of Nature and Environmental Technology, Division of Marine Environmental Studies, Kanazawa University, Housu-gun, Ishikawa 927-0553, Japan
[2]Bioorganic Research Institute, Suntory Foundation for Life Sciences, 8-1-1, Seikadai, Seika-cho, Soraku-gun, Kyoto, 619-0284, Japan
[3]Frontier Science Research Center, University of Miyazaki, Miyazaki, Miyazaki 889-1692, Japan
[4]National Institute for Basic Biology, Laboratory of Morphogenesis, 38 Nishigonaka Myodaiji, Okazaki 444-8585, Japan
[5]Institute of Noto SATOUMI Education and Studies, Noto-cho, Ishikawa 927-0553, Japan
[6]Department of Animal Bioscience, Faculty of Bioscience, Nagahama Institute of Bio-Science and Technology, Nagahama, Shiga 526-0829, Japan
[7]Department of Marine Biosciences, Division of Marine Science, Tokyo University of Marine Science and Technology, Minato-ku, Tokyo 108-8477, Japan
[8]Department of Biology, College of Liberal Arts and Sciences, Tokyo Medical and Dental University, Ichikawa, Chiba 272-0827, Japan
[9]Department of Zoology, D.D.U. Gorakhpur University, Gorakhpur 273-009, India

*Address correspondence to: Dr. N. Suzuki, Noto Marine Laboratory, Institute of Nature and Environmental Technology, Division of Marine Environmental Studies, Kanazawa University, Ogi, Noto-cho, Ishikawa 927-0553, Japan. Tel: 81-768-74-1151; Fax: 81-768-74-1644;
E-mail: nobuos@staff.kanazawa-u.ac.jp

Highlights

• Amphioxus, *Branchiostoma floridae*, possesses three calcitonin (CT) family peptides designated as *B. floridae* CT family peptides 1–3 (Bf-CTFP1–3).

• Bf-CTFPs suppress the ostoclastic activity of goldfish scales *via* the CT receptor.

• Bf-CTFPs and salmon CT share common essential amino acids for ligand activity.

• The alpha-helical structure of Bf-CTFP1 and 2 is conserved with that of teleost CT.

• Bf-CTFP3 has a unique alpha-helical structure.

Abstract

Calcitonin (CT) is a hormone which decreases serum calcium level by suppression ofosteoclastic activity in the vertebrate bone. In vertebrates, the structure-function relationship of CTs has been studied extensively. We recently identified three CT superfamily peptides, Bf-CTFP1 to 3, and uncovered the molecular and functional characteristics of their receptor and receptor activity-modifying protein in amphioxus, *Branchiostoma floridae*. However, the CT activity of Bf-CTFPs has yet to be investigated. In the present study, a functional analysis of Bf-CTFPs was performed using goldfish scales having both osteoclasts and osteoblasts. All Bf-CTFPs suppressed osteoclastic activity *via* a goldfish CT receptor. Although the primary amino acid sequences of the Bf-CTFPs showed low sequence similarity to vertebrate CTs, Bf-CTFP1 to 3 share three amino acids, Thr^{25}, Thr^{27}, and Pro^{32}-NH_2, that are required for receptor binding, with salmon CT. Moreover, homology model analysis revealed that the Bf-CTFPs form alpha-helical structure. The alpha-helical position and length of Bf-CTFP1 and 2 were conserved with those of a highly potent ligand, teleost CT. Interestingly, the position and length of the alpha-helix of Bf-CTFP3 differed from those of teleost CT and non-potent ligand (mutated salmon CT), despite that the action of Bf-CTFP3 on goldfish scales was the same as that of Bf-CTFP1 and 2. Collectively, the present study provides new insights into the structure-function relationship of CT and its functional evolution in chordates.

Keywords

Calcitonin, amphioxus, structure-activity relationship, alpha-helix, goldfish scales

1. Introduction

Calcitonin (CT) is a 32-amino acid peptide that has been identified from a wide range of vertebrates, except cyclostomes (Lafont et al., 2007; Sakamoto et al., 2000; Sexton et al., 1999; Suzuki et al., 1997). CT is mainly synthesized in C-cells of the thyroid gland in mammals and the ultimobranchial gland in non-mammalian species (Hull et al., 1998). In mammals, CT decreases the serum calcium level as a hypocalcemic hormone. CT suppresses bone resorption by inhibiting osteoclastic activity and modulates calcium excretion from the kidney (Hirsch et al., 2001; Horne et al., 1994). These CT functions are mediated by the CT receptor (CTR), which is a secretin type G-protein coupled receptor and possesses a long N-terminal extracellular region, containing the hormone-binding domain (Martins et al., 2014). The structure-function relationship between CT and the CTR has been studied extensively. CT includes an N-terminal circular region formed by a disulfide bond between Cys^{1} and Cys^{7}, an alpha-helical region, and a loop region (Meyer et al., 1991). The alpha-helical and loop regions bind to the N-terminal extracellular region of the CTR, whereas the N-terminal circular region interacts with the transmembrane domain of the CTR and is associated with CTR activation (Hoare, 2005; Watkins et al., 2012).

We recently clarified the molecular and functional characteristics of the CT superfamily peptides, their authentic receptor, and the receptor activity-modifying protein (RAMP) in amphioxus, *Branchiostoma floridae* (Sekiguchi et al., 2016). In vertebrates, CT superfamily peptides, including CT, CT gene-related peptide, adrenomedullin (AM), amylin, and CT receptor-stimulating peptide, are involved in bone metabolism, vasodilation, regulation of blood pressure, glucose metabolism, and food intake regulation, respectively (Brain et al., 1993; Cooper et al., 1988; Kitamura et al., 1993; Sawada et al., 2006). These functions are mediated by the CTR or CTR-like receptor (CLR) (Martins et al., 2014). The receptor specificity of CT superfamily peptides is determined by the combination of CTR/CLR and 3 types of RMAP (Bomberger et al., 2012). Furthermore, RAMP is involved in the cell surface translocation of CLR (Bomberger et al., 2012). The amphioxus CT superfamily peptides, designated as Bf-CTFPs, activate the heterodimeric Bf-CTFP receptor (Bf-CTFP-R) and RAMP-like protein (Bf-RAMP-LP). However, the monomeric Bf-CTFP-R was not activated by Bf-CTFPs due to the lack of cell-surface expression. Accordingly, we have revealed the prototypical molecular function of CT superfamily in chordates, whereas the biological function of Bf-CTFPs remains unclear.

In the present study, to gain insights into the biological function of Bf-CTFPs, a functional analysis was performed using cultured goldfish scales, which is a model system used to study the function of CT (Suzuki et al., 2000). Furthermore, the primary and secondary structures of the Bf-CTFPs were elucidated by amino acid sequence comparison and homology modeling predictions, respectively. We found an evolutionarily conserved and unique CT structure-activity relationship in amphioxus. Our findings provide new insights into the evolution of the structure-function relationship of the CT family peptides in chordates.

2. Material and Methods

2.1. Animals

Goldfish (*Carassius auratus*) were purchased from the Higashikawa Fish Farm (Yamatokoriyama, Japan). Female and male Goldfish (20−30 g) were used for artificial fertilization in the Graduate School of Marine Science and Technology, Tokyo University of Marine Science and Technology. After the hatched fish grew to 12–15 cm in body length, they were moved to the Noto Marine Laboratory in Kanazawa University and used for in-vitro bioassays. All experimental procedures were conducted in accordance with the Guide for the Care and Use of Laboratory Animals prepared by Kanazawa University.

2.2. Effects of Bf-CTFPs on osteoclastic activities using cultured regenerating goldfish scales

Goldfish were anesthetized with ethyl 3-aminobenzoate methanesulfonic acid (Sigma-Aldrich, St. Louis, MO, USA). Eight normally developed scales around the lateral line of both sides were removed to initiate scale regeneration (Yachiguchi et al., 2014). On day 14, the goldfish were again anesthetized and the regenerating scales were removed from both sides. The eight scales obtained from the left side were incubated for 6 h in Leibovitz's L-15 medium (Invitrogen, Grand Island, NY, USA) containing a 1% penicillin-streptomycin mixture (ICN Biomedical, Aurora, OH, USA) supplemented with 10^{-8} or 10^{-6} M Bf-CTFPs synthesized in the previous study (Sekiguchi et al., 2016). The effects of Bf-CTFPs on the osteoclasts were estimated by the measurement of tartrate-resistant acid phosphatase (TRAP) activity (Suzuki et al., 2000; Thamamongood et al., 2012). The mean for TRAP activity (obtained from 8 individual scales of one goldfish) was compared with that of the scales from the right side (control untreated group). TRAP activities between the left and right side scales around the

lateral line in the same individual were almost similar by 48 h in culture (Omori et al., 2012; Yachiguchi et al., 2014).

2.3. Effect of a CT antagonist on the suppression of osteoclastic activity by Bf-CTFP treatment

To confirm that Bf-CTFPs activate the goldfish CTR specifically, 10^{-8} and 10^{-6} M Bf-CTFP1-3 were incubated the scales along with 10^{-8} and 10^{-6} M of a CTR antagonist (the 8–32 fragment of salmon CT (GenScript, Piscataway Township, NJ, USA) for 6 h. After incubation, TRAP activity in the scales was then measured using previously described methods (Yachiguchi et al., 2014). The mean for TRAP activity following Bf-CTFP1-3 treatment (obtained from 8 individual scales from one goldfish) was compared with that of the right side (control untreated group).

2.4. Homology modeling of Bf-CTFPs

The Bf-CTFP1-3 sequences were aligned with that of salmon CT (PDB ID: 2GLG and 2GLH), human CT (PDB ID: 2JXZ), and human AM (PDB ID: 2L7S), using Clustal W (Andreotti et al., 2006; Perez-Castells et al., 2012). Salmon CT (PDB ID: 2GLG) is a mutant in which Pro^{23} and Leu^{24} of wild type CT is substituted by Arg^{23} and Ala^{24}, respectively. The mutant possesses a longer alpha-helical region and exhibits a lower binding affinity and potency compared with wild type salmon CT (Andreotti et al., 2006). MODELLER 9.16 (Webb and Sali, 2014) was used to build the homologous models. For each peptide, 1000 models were created by introducing a disulfide restraint between conserved cysteines. The output structures were scored with DOPE score and the five lowest scored structures were selected for each peptide. Amidation of the C-terminus and energy minimization were performed with the CHARMM force field in Discovery Studio 3.5.1 (Accelrys, Burlington, MA, USA). To validate the structures, 10 ns equilibration in water was performed with GROMACS 4.6.1 (Hess et al.). The image for the structure with the lowest potential energy in GROMACS equilibration was visualized using the graphics program Chimera 11.10.1 (Pettersen et al., 2004).

2.5. Statistical analysis

All results are represented as the means ± SEM (n = 8). The statistical significance between the control and experimental groups was estimated by the paired *t*-test.

3. Results

3.1. Effects of Bf-CTFPs on osteoclastic activities using cultured goldfish scales

To evaluate the suppression of osteoclastic activity by Bf-CTFPs, we performed the TRAP assay. Treatment of goldfish scales with 10^{-8} M Bf-CTFPs for 6 h resulted in significant suppression of TRAP activity ($P < 0.01$) (Fig. 1A). This significant suppressive effect was also observed with 10^{-6} M Bf-CTFPs ($P < 0.01$) (Fig. 1A, B). At 10^{-9} M, none of the Bf-CTFPs affected TRAP activity in the goldfish scales (data not shown). The suppressive effect was similar between all Bf-CTFP peptides (Fig. 1A, B).

No effect of antagonist alone treatment on osteoclastic activity was detected (data not shown).

3.2. Analysis of Bf-CTFP specificity to CTR using a calcitonin antagonist

CT possesses two functional domains: the N-terminal circular region and the region following circular region, which are the receptor-activated domain and receptor-binding domain, respectively (Watkins et al., 2012). Because of the occupation of the receptor with no activity, N-terminal-truncated CT is often used as an antagonist of CTR. To evaluate whether the Bf-CTFPs function specifically through binding to the goldfish CTR, we performed TRAP assay in the presence of the N-terminal truncated salmon CT antagonist. The suppressive effect of 10^{-8} and 10^{-6} M Bf-CTFPs on TRAP activity was inhibited by this treatment (Fig. 2A, B).

3.3. Primary sequence comparison between Bf-CTFPs and vertebrate CTs

To elucidate functional similarities between Bf-CTFPs and vertebrate CTs, we compared their primary amino acid sequences (Fig. 3). The sequence similarities of Bf-CTFP1, 2, and 3 to vertebrate CTs were 29.4–50, 33.3–38.9, and 26.5–41.2%, respectively (Table 1). The similarities between amphioxus and vertebrates were lower than those between human and teleosts (Table 1). The N-terminal circular region of all Bf-CTFPs formed by 6 amino acids showed similarity with that of human AM rather than vertebrate CTs (Fig. 3). In the region following the N-terminal circular region, four amino acids, Thr^{25}, Thr^{27}, Gly^{28}, and Pro^{32}-NH_2, important for receptor-binding and truncated in the salmon CT antagonist, salmon CT–(22–32) (Lee et al., 2016), were conserved in Bf-CTFP2 (Thr^{25}, Thr^{27}, Gly^{28}, and Pro^{33}-NH_2) and Bf-CTFP3 (Thr^{23}, Thr^{25}, Gly^{26}, and Pro^{31}-NH_2). However, in Bf-CTFP1, three C-terminal amino acids (Thr^{23}, Thr^{25}, and Pro^{31}-NH_2) were conserved with that of salmon CT–(22–32) (Thr^{25}, Thr^{27}, and Pro^{32}-NH_2) (Fig. 3).

3.4. Homology modeling analysis of Bf-CTFPs, salmon CT, and human AM

To gain insights into the structure-function relationship of Bf-CTFPs, we predicted their thermodynamically stable tertiary structure using the multiple template-based modeling software, MODELLER. The structures of wild type salmon CT (PDBID: 2GLH), eel CT (PDBID: 1BKU), human CT (PDBID: 1JZX), human AM (PDBID: 2L7S), and salmon CT with mutations (PDBID: 2GLG), which has a longer alpha-helix and shows lower affinity and potency than wild type salmon CT, were selected as templates. We defined the N-terminal, central, and C-terminal regions from salmon CT by NMR analysis (Fig. 4A) (Andreotti et al., 2006). The N-terminal region is covered by a ring structure between Cys^{1} and Cys^{7}. The central region that forms the alpha helical structure, and the C-terminal region that forms the flexible loop, are between V^{8} and T^{21}, and Y^{22} and P^{32}, respectively. The homology model estimations for all Bf-CTFPs revealed alpha-helical structures in the central region and loop domain in the C-terminus (Table 2 and Fig. 4A, 4B-d, 4B-h, and 4B-l). The number and length of alpha-helices of Bf-CTFP1 and 2 were similar to those of wild-type salmon CT (Table 2 and Fig. 4A, 4B-d, 4B-e, 4B-h, and 4B-i). However, the alpha-helical region of mutated salmon CT was longer than that of Bf-CTFP1 and 2 (Table 2 and Fig. 4A, 4B-f, and 4B-j). Furthermore, the number and length of Bf-CTFP1 and 2 were different from human AM that does not bind the CTR (Table 2 and Fig. 4A, 4B-g, and 4B-k). Bf-CTFP3 possessed two alpha-helices in the central region (Table 2 and Fig. 4A, 4B-l). Although the length of the region, including two alpha-helices, was similar to that of teleost CT, Bf-CTFP3 had a 3-amino acid loop structure in the central region (Table 2 and Fig. 4A and 4B-m). In addition, although human AM, an inactive ligand of the CTR, possessed the two alpha-helices, the length and position of the alpha-helical region were completely different from that of Bf-CTFP3. Especially, the second alpha-helix of human AM was located in the C-terminal region, unlike the second helix of Bf-CTFP3 that was located in the central region (Table 2 and Fig. 4A and 4B-o).

4. Discussion

In vertebrates, CT superfamily peptides and their receptors comprise various paralogous genes. The CT superfamily receptor has two types: CTR and CLR. Since the combination of CT superfamily peptides and their receptors is complex, the conformation of the peptide-receptor recognition has been studied extensively (Hoare, 2005; Meyer et al., 1991).

In the present study, we focused on the structure-function relationship of the amphioxus CT superfamily peptide, Bf-CTFP. We first performed functional analyses of the Bf-CTFPs using goldfish scales. Treatment with 10^{-8} M Bf-CTFPs significantly suppressed the osteoclastic activity of the scales (Fig. 1). In a previous study, we demonstrated that 10^{-9} M salmon CT significantly suppressed the osteoclastic activity in a goldfish scale culture system (Sekiguchi et al., 2009). The active concentration of Bf-CTFPs was relatively higher than that of salmon CT. This may be related to the different structures of the N-terminal circular form of Bf-CTFPs and vertebrate CTs, showing lower activity of Bf-CTFPs (Fig. 3). Moreover, Bf-CTFP activity was inhibited by treatment with a salmon CT antagonist, proving that Bf-CTFPs bind specifically to the goldfish CTR (Fig. 2). Collectively, these data confirmed that CT-like activity is conserved in amphioxus CT superfamily peptides.

The results of the primary sequence comparison suggested that Bf-CTFPs were a hybrid peptide consisting of vertebrate AM-like and CT-like sequences. The N-terminal circular region resembled that of vertebrate AM, whereas the central and C-terminal regions showed similarity with CT (Fig. 3). Furthermore, amino acid sequence similarities between Bf-CTFPs and vertebrate CTs were less than similarities among vertebrate CTs (Table 1). In contrast, the four C-terminal residues, including Thr^{25}, Thr^{27}, Gly^{28}, and Pro^{33}-NH_2 of Bf-CTFP2, and Thr^{23}, Thr^{25}, Gly^{26}, and Pro^{31}-NH_2 of Bf-CTFP3, were conserved when compared to that of salmon CT (Thr^{25}, Thr^{27}, Gly^{28}, and Pro^{32}-NH_2) (Fig. 3). These amino acids are responsible for the CTR binding of salmon CT–(22–32), implying that Bf-CTFP2 and 3 possess a CTR binding mechanism similar to that of salmon CT. In Bf-CTFP1, three amino acids (Thr^{23}, Thr^{25}, and Pro^{31}-NH_2) were the same as those of the salmon CT antagonist (Thr^{25}, Thr^{27}, and Pro^{32}-NH_2). However, Gly^{28} in salmon CT was substituted by Ala^{26} in Bf-CTFP1. In salmon CT–(22–32), the Gly^{25} residue is associated with the flexibility of this fragment. Thus, this residue is likely necessary for the interaction between the CTR and the C-terminal Pro^{32}-NH_2 of salmon CT–(22–32). Bf-CTFP1 has five amino acids (Asn^{27}, Pro^{28}, Tyr^{29}, Ser^{30}, and Pro^{31}) after Ala^{26}, all of which are involved in the flexible loop structure (Li et al., 2006). Taken together, these results suggest that a binding motif of salmon CT is conserved in a common ancestor of teleosts and amphioxus.

Prediction of the secondary structure by homology model analysis revealed that Bf-CTFPs possess an alpha-helix in the central region of the peptides (Table 2 and Fig. 4A, 4B-d, 4B-h, and 4B-l). NMR and circular dichroism analyses demonstrated that alpha-helical regions are present in the central position of vertebrate CT (Castiglione Morelli et al., 1992; Meadows et al., 1991; Meyer et al., 1991; Motta et al., 1991). A comparative study of the

structure-activity relationship between native and mutant CT indicates that the length of the alpha-helical region is responsible for CT activity (Andreotti et al., 2006), suggesting that the alpha helical structure negatively affects the binding motif (Thr^{25}, Thr^{27}, Gly^{28}, and Pro^{32}-NH_2) in the C-terminal region. In addition, photoaffinity labeling assays using salmon CT indicates that the alpha-helical region interacts with the N-terminal region of the CTR (Dong et al., 2004; Pham et al., 2004). The current homology modeling analysis demonstrated that the length and position of the alpha-helix in Bf-CTFP1 and 2 is comparable to that of salmon and eel CT, which exhibit higher activity (Hoare, 2005; McDermott and Kidd, 1987), but not to that of human CT, which shows a lower activity (Table 2). These findings suggest that the interaction properties of Bf-CTFP1 and 2 with goldfish CTR are similar to those of teleost CTs (Table 2, 4A, 4B-e, and 4B-i). The functional analysis using the goldfish scale system supports this notion (Fig. 1 and 2). However, the thermodynamically stable structure of Bf-CTFP3 is different from that of Bf-CTFP1 and 2; nevertheless, they all show similar activities in the cultured goldfish scale system. This finding suggests that Bf-CTFP3 functions with the goldfish CTR in two possible modes of action. One possibility is that the CTR-binding conformation of Bf-CTFP3 is similar to that of Bf-CTFP1 and 2. This is in good agreement with the fact that Bf-CTFP3 shares the same residues that are required for CTR binding with the salmon CT antagonist (Fig. 3). The other explanation is that another CTR-binding conformation exists in Bf-CTFP3.

In a previous study, we demonstrated the suppression of osteoclastic activity of a CT-like peptide in the ascidian, *Ciona intestinalis*, using a goldfish scale culture system (Sekiguchi et al., 2009). *Ciona* CT (Ci-CT) significantly and dose-dependently suppressed TRAP activity in cultured goldfish scales. Furthermore, Ci-CT possessed the alpha-helical region like vertebrate CT. However, the C-terminal residues of Ci-CT (Gln^{24}, Val^{26}, Gly^{27}, and Pro^{30}-NH_2) were different from those of salmon CT (Thr^{25}, Thr^{27}, Gly^{28}, and Pro^{32}-NH_2) (Fig. 3). The substitutions, Thr/Gln and Thr/Val, were detected between ascidian and salmon CT. The Val residue presents a similar amino acid side chain with Thr residues, and substitution of Thr/Val is widely observed in teleosts. Therefore, the replacement of Thr^{25} in salmon CT with Gln^{24} in ascidian CT is considered the most critical substitution. Vertebrates also present differences in terms of key amino acids for CTR binding compared to salmon CT. In cetartiodactyla including cow, pig, and whales, CT activates the CTR even though CTR-interacting residues are not conserved (Sasayama et al., 1992). For example, porcine CT possesses Met^{25}, Phe^{27}, Gly^{28}, and Pro^{32}-NH_2 in the C-terminal region (Sasayama et al., 1992). Moreover, human and rat CT present

a motif composed of Thr^{25}, Ile^{27}, Gly^{28}, and Pro^{32}-NH_2. These findings imply that vertebrate CT peptides possess at least three types of conformation for the binding and activation of the receptor. Altogether, amino acid differences observed in Ci-CT and Bf-CTFP1 suggest that they bind and activate CTR with different conformations from vertebrate CTs.

In the present study, we performed a CT assay using goldfish scales. Teleost fish scale is a dermal skeleton that includes osteoblast, osteoclast, and the bone matrix (Bereiter-Hahn and Zylberberg, 1993; Sire and Akimenko, 2004). In zebrafish, sea bream, and goldfish, scale assay has been established (de Vrieze et al., 2014; Redruello et al., 2005; Suzuki and Hattori, 2002). The assay is suitable for interaction between osteoblast and osteoclast. Furthermore, goldfish culture system shows the high sensitivity and selectivity. CT was effective at 10^{-11} M for 18 h and did not affect osteoblastic activity (Sekiguchi et al., 2016; Suzuki et al., 2009). Therefore, goldfish scale culture system has been regarded as an excellent model for studying the effect of hormones and pollutants on bone homeostasis (Suzuki et al., , 2000; Suzuki and Hattori, 2002; Suzuki et al., 2004; Yachiguchi et al., 2014). The present study shows that this system can also be used to assess the functions of invertebrate CT-like peptides. To date, CT-like peptides have been identified and predicted in invertebrate deuterostomes such as acorn worm, sea urchin, sea star, and sea cucumber and protostomes such as polychaete and owl limpet (Rowe et al., 2014; Rowe and Elphick, 2012; Semmens et al., 2016). Using this system to analyze CT-like peptides might allow us to gain insights into the evolution of the structure-activity relationship in metazoan.

In conclusion, we found that CT/CGRP family peptides of amphioxus possess typical CT bioactivities and form functional structures both unique and similar to those of vertebrate CT. These results suggest that the teleost CT-type active structure is the most primitive type in chordate CTs. This study paves the way for investigation of the unprecedented structure-function relationship and evolutionary aspects of the CT family peptides in chordates.

Competing Interests

The authors have no competing interest to declare.

Acknowledgments

This study was supported in part by grants to T.S. (Scientific Research [C] No. 15K07126 by JSPS), to N.S. (Grant-in-Aid for Scientific Research [C] No. 16K07871 by JSPS), and to A.H.

(Grant-in-Aid for Scientific Research [C] No. 24570068 by JSPS). This study was conducted as part of the cooperative research program of the Institute of Nature and Environmental Technology, Kanazawa University < Accept No. 13 >.

References

Andreotti, G., Mendez, B.L., Amodeo, P., Morelli, M.A., Nakamuta, H., Motta, A., 2006. Structural determinants of salmon calcitonin bioactivity: the role of the Leu-based amphipathic alpha-helix. J. Biol. Chem. 281, 24193-24203.

Bereiter-Hahn, J., Zylberberg, L., 1993. Regeneration of teleost fish scale. Comp. Biochem. Physiol. A. Physiol. 105, 625-641.

Bomberger, J.M., Parameswaran, N., Spielman, W.S., 2012. Regulation of GPCR trafficking by RAMPs. Adv. Exp. Med. Biol. 744, 25-37.

Brain, S.D., Hughes, S.R., Cambridge, H., O'Driscoll, G., 1993. The contribution of calcitonin gene-related peptide (CGRP) to neurogenic vasodilator responses. Agents Actions 38 Spec No, C19-21.

Castiglione Morelli, M.A., Pastore, A., Motta, A., 1992. Dynamic properties of salmon calcitonin bound to sodium dodecyl sulfate micelles: a restrained molecular dynamics study from NMR data. J. Biomol. NMR 2, 335-348.

Cooper, G.J., Leighton, B., Dimitriadis, G.D., Parry-Billings, M., Kowalchuk, J.M., Howland, K., Rothbard, J.B., Willis, A.C., Reid, K.B., 1988. Amylin found in amyloid deposits in human type 2 diabetes mellitus may be a hormone that regulates glycogen metabolism in skeletal muscle. Proc. Natl. Acad. Sci. U. S. A. 85, 7763-7766.

de Vrieze, E., Moren, M., Metz, J.R., Flik, G., Lie, K.K., 2014. Arachidonic acid enhances turnover of the dermal skeleton: studies on zebrafish scales. PLoS One 9, e89347.

Dong, M., Pinon, D.I., Cox, R.F., Miller, L.J., 2004. Importance of the amino terminus in secretin family G protein-coupled receptors. Intrinsic photoaffinity labeling establishes initial docking constraints for the calcitonin receptor. J. Biol. Chem. 279, 1167-1175.

Hess, B., Kutzner, C., van der Spoel, D., Lindahl, E., 2008. GROMACS 4: Algorithms for Highly Efficient, Load-Balanced, and Scalable Molecular Simulation. J. Chem. Theory Comput. 4, 435-447.

Hirsch, P.F., Lester, G.E., Talmage, R.V., 2001. Calcitonin, an enigmatic hormone: does it have a function? J. Musculoskelet. Neuronal Interact. 1, 299-305.

Hoare, S.R., 2005. Mechanisms of peptide and nonpeptide ligand binding to Class B G-protein-coupled receptors. Drug Discov. Today 10, 417-427.

Horne, W.C., Shyu, J.F., Chakraborty, M., Baron, R., 1994. Signal transduction by calcitonin Multiple ligands, receptors, and signaling pathways. Trends Endocrinol. Metab. 5, 395-401.

Hull, K.L., Fathimani, K., Sharma, P., Harvey, S., 1998. Calcitropic peptides: neural perspectives. Comp. Biochem. Physiol. C Pharmacol. Toxicol. Endocrinol. 119, 389-410.

Kitamura, K., Kangawa, K., Kawamoto, M., Ichiki, Y., Nakamura, S., Matsuo, H., Eto, T., 1993. Adrenomedullin: a novel hypotensive peptide isolated from human pheochromocytoma. Biochem. Biophys. Res. Commun. 192, 553-560.

Lafont, A.G., Dufour, S., Fouchereau-Peron, M., 2007. Evolution of the CT/CGRP family: comparative study with new data from models of teleosts, the eel, and cephalopod molluscs, the cuttlefish and the nautilus. Gen. Comp. Endocrinol. 153, 155-169.

Lee, S.M., Hay, D.L., Pioszak, A.A., 2016. Calcitonin and Amylin Receptor Peptide Interaction Mechanisms: Insights into peptide-binding modes and allosteric modulation of the calcitonin receptor by receptor activity-modifying proteins. J. Biol. Chem. 291, 8686-8700.

Li, Z.R., Lin, H.H., Han, L.Y., Jiang, L., Chen, X., Chen, Y.Z., 2006. PROFEAT: a web server for computing structural and physicochemical features of proteins and peptides from amino acid sequence. Nucleic Acids Res. 34, W32-37.

Martins, R., Vieira, F.A., Power, D.M., 2014. Calcitonin receptor family evolution and fishing for function using in silico promoter analysis. Gen. Comp. Endocrinol. 209, 61-73.

McDermott, M.T., Kidd, G.S., 1987. The role of calcitonin in the development and treatment of osteoporosis. Endocr. Rev. 8, 377-390.

Meadows, R.P., Nikonowicz, E.P., Jones, C.R., Bastian, J.W., Gorenstein, D.G., 1991. Two-dimensional NMR and structure determination of salmon calcitonin in methanol. Biochemistry 30, 1247-1254.

Meyer, J.P., Pelton, J.T., Hoflack, J., Saudek, V., 1991. Solution structure of salmon calcitonin. Biopolymers 31, 233-241.

Motta, A., Pastore, A., Goud, N.A., Castiglione Morelli, M.A., 1991. Solution conformation of salmon calcitonin in sodium dodecyl sulfate micelles as determined by two-dimensional NMR and distance geometry calculations. Biochemistry 30, 10444-10450.

Omori, K., Wada, S., Maruyama, Y., Hattori, A., Kitamura, K., Sato, Y., Nara, M., Funahashi, H., Yachiguchi, K., Hayakawa, K., Endo, M., Kusakari, R., Yano, S., Srivastav, A.K.,

Kusui, T., Ejiri, S., Chen, W., Tabuchi, Y., Furusawa, Y., Kondo, T., Sasayama, Y., Nishiuchi, T., Nakano, M., Sakamoto, T., Suzuki, N., 2012. Prostaglandin E(2) increases both osteoblastic and osteoclastic activity in the scales and participates in calcium metabolism in goldfish. Zoolog. Sci. 29, 499-504.

Perez-Castells, J., Martin-Santamaria, S., Nieto, L., Ramos, A., Martinez, A., Pascual-Teresa, B., Jimenez-Barbero, J., 2012. Structure of micelle-bound adrenomedullin: a first step toward the analysis of its interactions with receptors and small molecules. Biopolymers 97, 45-53.

Pettersen, E.F., Goddard, T.D., Huang, C.C., Couch, G.S., Greenblatt, D.M., Meng, E.C., Ferrin, T.E., 2004. UCSF Chimera--a visualization system for exploratory research and analysis. J. Comput. Chem. 25, 1605-1612.

Pham, V., Wade, J.D., Purdue, B.W., Sexton, P.M., 2004. Spatial proximity between a photolabile residue in position 19 of salmon calcitonin and the amino terminus of the human calcitonin receptor. J. Biol. Chem. 279, 6720-6729.

Redruello, B., Estevao, M.D., Rotllant, J., Guerreiro, P.M., Anjos, L.I., Canario, A.V., Power, D.M., 2005. Isolation and characterization of piscine osteonectin and downregulation of its expression by PTH-related protein. J. Bone Miner. Res. 20, 682-692.

Rowe, M.L., Achhala, S., Elphick, M.R., 2014. Neuropeptides and polypeptide hormones in echinoderms: new insights from analysis of the transcriptome of the sea cucumber Apostichopus japonicus. Gen. Comp. Endocrinol. 197, 43-55.

Rowe, M.L., Elphick, M.R., 2012. The neuropeptide transcriptome of a model echinoderm, the sea urchin Strongylocentrotus purpuratus. Gen. Comp. Endocrinol. 179, 331-344.

Sakamoto, H., Sasayama, Y., Ueda, K., 2000. Anuran Calcitonins are Diverse in Lower Vertebrates. Zoolog. Sci. 17, 97-101.

Sasayama, Y., Suzuki, N., Oguro, C., Takei, Y., Takahashi, A., Watanabe, T.X., Nakajima, K., Sakakibara, S., 1992. Calcitonin of the stingray: comparison of the hypocalcemic activity with other calcitonins. Gen. Comp. Endocrinol. 86, 269-274.

Sawada, H., Yamaguchi, H., Shimbara, T., Toshinai, K., Mondal, M.S., Date, Y., Murakami, N., Katafuchi, T., Minamino, N., Nunoi, H., Nakazato, M., 2006. Central effects of calcitonin receptor-stimulating peptide-1 on energy homeostasis in rats. Endocrinology 147, 2043-2050.

Sekiguchi, T., Kuwasako, K., Ogasawara, M., Takahashi, H., Matsubara, S., Osugi, T., Muramatsu, I., Sasayama, Y., Suzuki, N., Satake, H., 2016. Evidence for Conservation of the Calcitonin Superfamily and Activity-regulating Mechanisms in the Basal Chordate

Branchiostoma floridae: INSIGHTS INTO THE MOLECULAR AND FUNCTIONAL EVOLUTION IN CHORDATES. J. Biol. Chem. 291, 2345-2356.

Sekiguchi, T., Suzuki, N., Fujiwara, N., Aoyama, M., Kawada, T., Sugase, K., Murata, Y., Sasayama, Y., Ogasawara, M., Satake, H., 2009. Calcitonin in a protochordate, Ciona intestinalis--the prototype of the vertebrate calcitonin/calcitonin gene-related peptide superfamily. FEBS J 276, 4437-4447.

Semmens, D.C., Mirabeau, O., Moghul, I., Pancholi, M.R., Wurm, Y., Elphick, M.R., 2016. Transcriptomic identification of starfish neuropeptide precursors yields new insights into neuropeptide evolution. Open Biol. 6, 150224.

Sexton, P.M., Findlay, D.M., Martin, T.J., 1999. Calcitonin. Curr. Med. Chem. 6, 1067-1093.

Sire, J.Y., Akimenko, M.A., 2004. Scale development in fish: a review, with description of sonic hedgehog (shh) expression in the zebrafish (Danio rerio). Int. J. Dev. Biol. 48, 233-247.

Suzuki, N., Eguchi, C., Hirai, T., Sasayama, Y., 1997. Nucleotide sequences of reptile calcitonins: their high homology to chicken calcitonin. Zoolog. Sci. 14, 833-836.

Suzuki, N., Hattori, A., 2002. Melatonin suppresses osteoclastic and osteoblastic activities in the scales of goldfish. J. Pineal Res. 33, 253-258.

Suzuki, N., Suzuki, T., Kurokawa, T., 2000. Suppression of osteoclastic activities by calcitonin in the scales of goldfish (freshwater teleost) and nibbler fish (seawater teleost). Peptides 21, 115-124.

Suzuki, N., Yamamoto, M., Watanabe, K., Kambegawa, A., Hattori, A., 2004. Both mercury and cadmium directly influence calcium homeostasis resulting from the suppression of scale bone cells: the scale is a good model for the evaluation of heavy metals in bone metabolism. J. Bone Miner. Metab. 22, 439-446.

Thamamongood, T.A., Furuya, R., Fukuba, S., Nakamura, M., Suzuki, N., Hattori, A., 2012. Expression of osteoblastic and osteoclastic genes during spontaneous regeneration and autotransplantation of goldfish scale: a new tool to study intramembranous bone regeneration. Bone 50, 1240-1249.

Watkins, H.A., Au, M., Hay, D.L., 2012. The structure of secretin family GPCR peptide ligands: implications for receptor pharmacology and drug development. Drug Discov. Today 17, 1006-1014.

Webb, B., Sali, A., 2014. Comparative Protein Structure Modeling Using MODELLER. Curr. Protoc. Bioinformatics 47, 5.6.1-32.

Yachiguchi, K., Matsumoto, N., Haga, Y., Suzuki, M., Matsumura, C., Tsurukawa, M., Okuno, T., Nakano, T., Kawabe, K., Kitamura, K., Toriba, A., Hayakawa, K., Chowdhury, V.S., Endo, M., Chiba, A., Sekiguchi, T., Nakano, M., Tabuchi, Y., Kondo, T., Wada, S., Mishima, H., Hattori, A., Suzuki, N., 2014. Polychlorinated biphenyl (118) activates osteoclasts and induces bone resorption in goldfish. Env. Sci. Poll. Res., 21, 6365–6372.

Figure Legends

Fig. 1. Effect of Bf-CTFPs on tartrate-resistant acid phosphatase (TRAP) activity in cultured regenerating goldfish scales. Scales were incubated with individual Bf-CTFPs for 6 h.
Double asterisks (**) indicate a significant difference at $P < 0.01$ compared to control scales. n = 8 samples; one sample per one fish.

Fig. 2. Effects of a CT antagonist on the inhibition of Bf-CTFPs using cultured regenerating goldfish scales. No significant difference was observed between experimental and control scales. n = 8 samples; one sample per one fish.

Fig. 3. Multiple alignments of Bf-CTFPs and vertebrate CTs.
Amino acid sequences of Bf-CTFP1-3 were compared with those of chordate CT and human AM: human CT (NP_001029124), salmon CT (AAM18088), eel CT (760596A), *Ciona* CT (BAI63095), Bf-CTFP1 (BAU51800), Bf-CTFP2 (BAU51801), Bf-CTFP3 (BAU51802), and human AM (AAB26458). Multiple alignments were estimated by using CLUSTAL X2 Multiple Sequence Alignment software. Identical and similar amino acid sequences among half of the total members are shown by the black and gray boxes, respectively.

Fig. 4. Homology modeling of Bf-CTFPs, salmon CT, mutated salmon CT, and human AM.
(A) Location of the N-terminal, central, and C-terminal regions is defined by salmon CT structural data. The alpha helix is shown by the red bar. The ‘a’ following each peptide sequence indicates the amide. (B) The structure of salmon CT (a), mutated salmon CT (b), human AM (c), Bf-CTFP1 (d), Bf-CTFP2 (h), and Bf-CTFP3 (l) was calculated by homology modeling. The alpha-helical structure of salmon CT, mutated salmon CT, and human AM is depicted by light blue. The alpha-helix of Bf-CTFPs is shown by red. Bf-CTFP1 was compared with salmon CT (e), mutated salmon CT (f), and human AM (g) in an overlapping manner. Bf-CTFP2 was compared with salmon CT (i), mutated salmon CT (j), human AM (k) in an overlapping manner. Bf-CTFP3 was compared with salmon CT (m), mutated salmon CT (n), and human AM (o) in an overlapping manner. The conserved alpha-helical region in salmon CT, eel CT, and human CT is depicted by two green lines.

Table 1. Amino acid sequence similarity (%) in chordate CTs

Multiple alignments of Bf-CTFPs and vertebrate CTs were performed by using BioEdit. Similarity was calculated by the pairwise alignment using the BLOSUM62 matrix.

	Bf-CTFP1	Bf-CTFP2	Bf-CTFP3	human CT	salmon CT
Bf-CTFP1					
Bf-CTFP2	47.1				
Bf-CTFP3	35.3	41.7			
human CT	29.4	33.3	26.5		
salmon CT	50	38.9	44.1	68.8	
eel CT	44.1	36.1	41.2	71.9	96.9

Table 2. Predicted alpha-helical structure in homology modeling analysis

Peptide	Number of helices	Distribution of helices	Resides
Bf-CTFP1	1	5–22	31
Bf-CTFP2	1	7–26	33
Bf-CTFP3	2	6–16, 20–24	33
salmon CT (WT)	1	4–21	32
salmon CT (mut)	1	5–30	32
eel CT	1	5–19	32
human CT	2	3–21, 25–28	32
human AM	2	22–31, 43–52	52

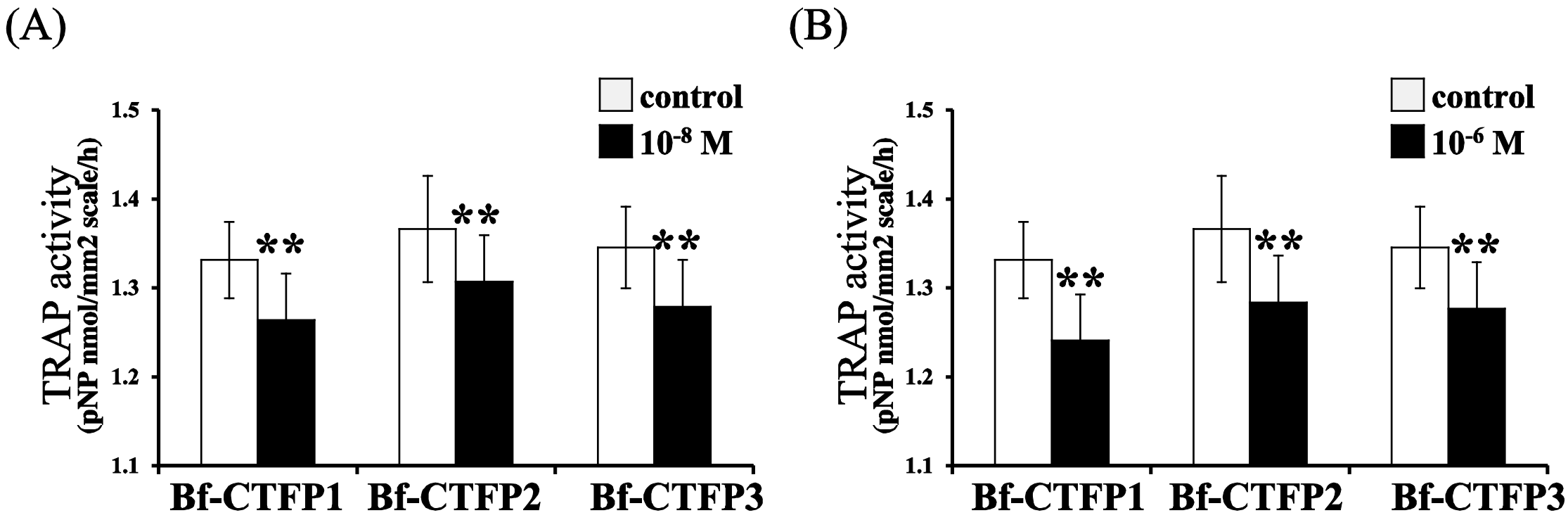

Fig. 1 Sekiguchi *et al.*

(A)

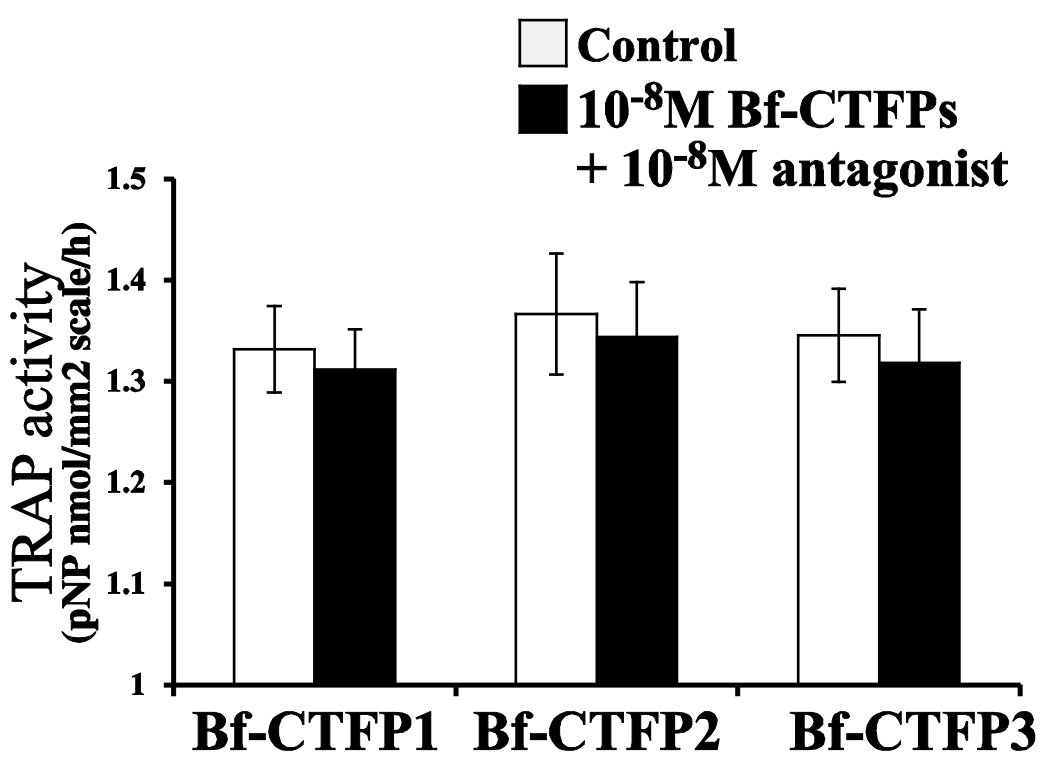

(B)

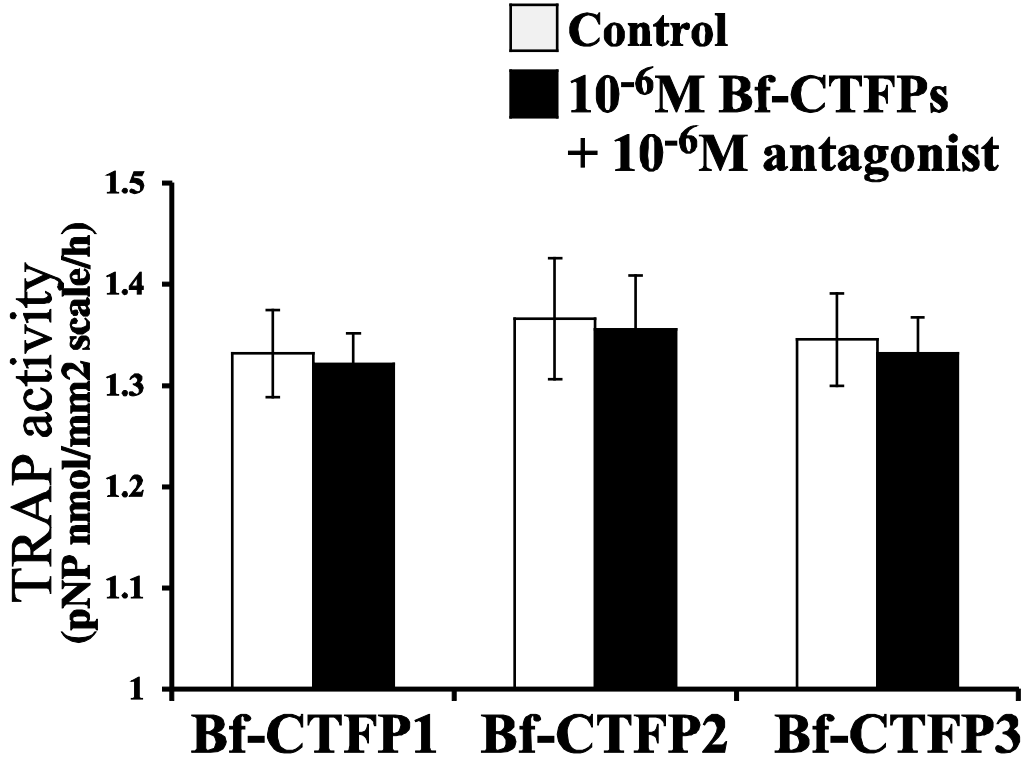

Fig. 2 Sekiguchi *et al.*,

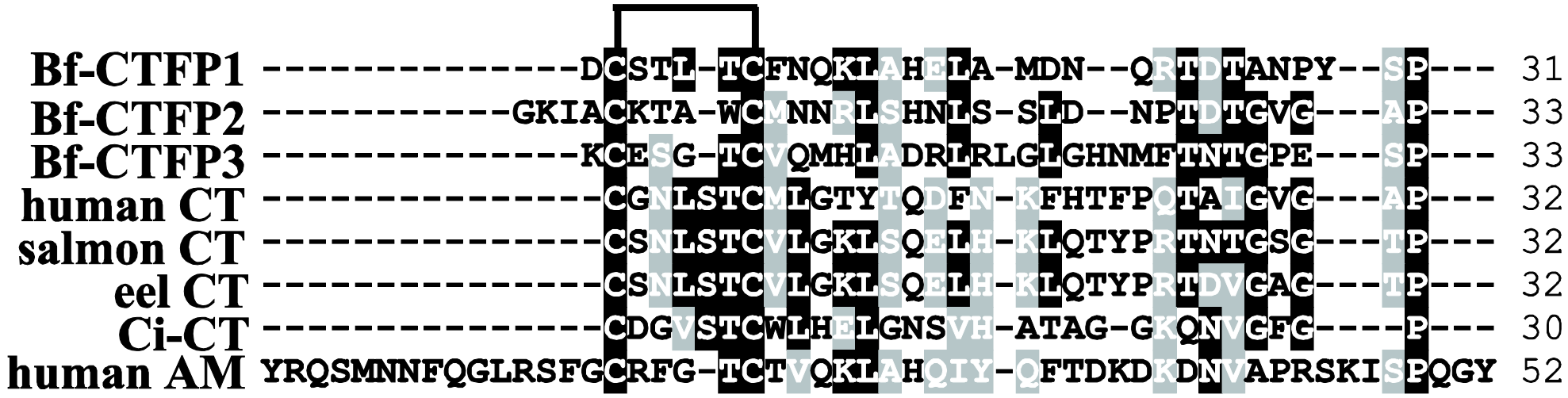

Fig. 3 Sekiguchi *et al.*,

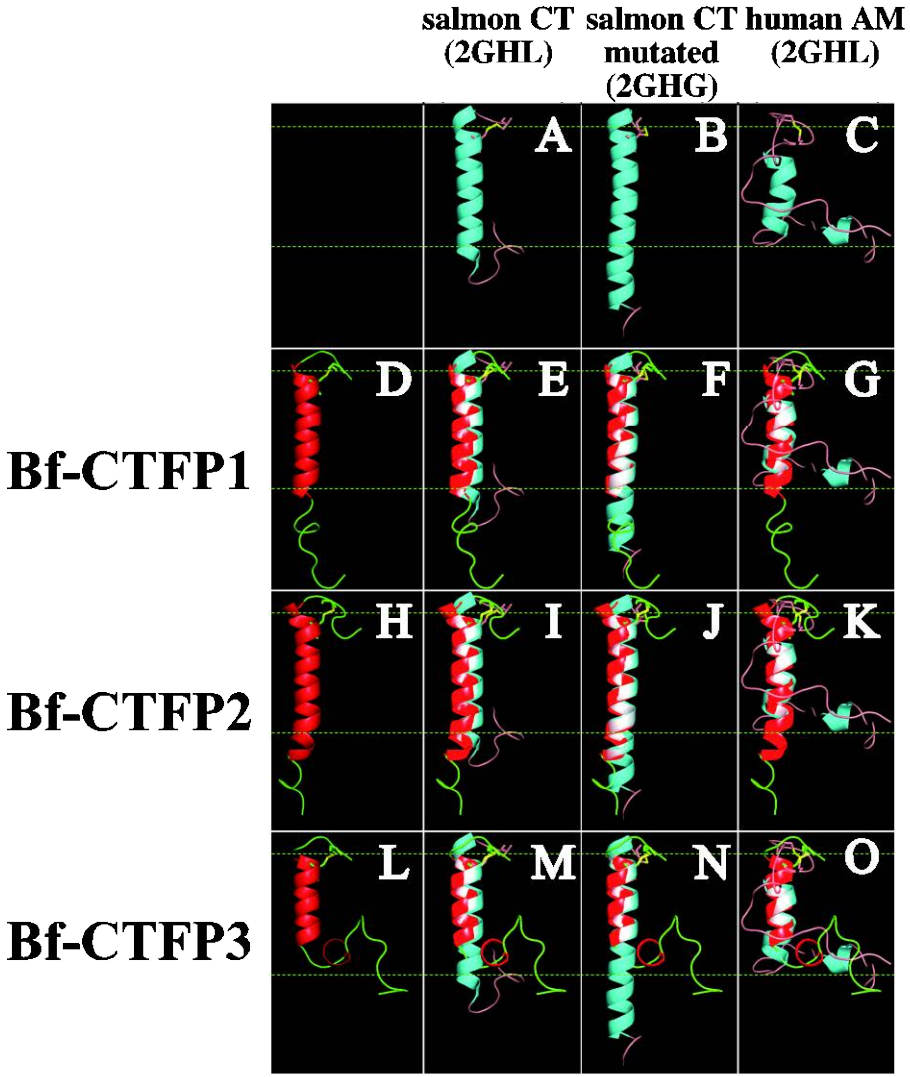

Fig. 4 Sekiguchi *et al.*,